

# The investigation of microstructure and mechanical properties of oxide powders coated on engine pistons surface

ERDİNÇ VURAL, SERKAN ÖZEL<sup>a,\*</sup>, BÜLENT ÖZDALYAN<sup>b</sup>

*Bitlis Eren University, Vocational School of Technical Sciences, 13000-Bitlis, Turkey*

<sup>a</sup>*Bitlis Eren University, Faculty of Engineering Architecture, Dept. of Mechanical Eng., 13000-Bitlis, Turkey*

<sup>b</sup>*Karabük University, Faculty of Engineering, Department of Automotive Engineering, 78100-Karabük, Turkey*

In this study, the surface of a piston (AlSi12CuNi) belonging to a diesel engine was coated with  $ZrO_2+MgO/Al_2O_3$  powders by using plasma spray technique. The coating layers were examined with optical microscopy, SEM, EDS and XRD analysis. The adhesive strength and microhardness were measured. In XRD studies, such compounds as  $ZrO_2$  (Tetragonal),  $ZrO_2$  (Monoclinic), MgO,  $Al_3Zr_5$ ,  $\alpha-Al_2O_3$  and  $\gamma-Al_2O_3$  have been identified on  $ZrO_2+MgO/Al_2O_3$  coating layers. The best adhesion strength and maximum hardness value have been determined in the sample coated with  $ZrO_2+MgO+50wt. \%Al_2O_3$  powder.

(Received April 2, 2014; accepted May 15, 2014)

*Keywords:* Piston, Plasma Spraying, Coating,  $ZrO_2 + MgO / Al_2O_3$

## 1. Introduction

Research and technological innovation studies aiming to reduce fuel consumption and reduce the cost in motor vehicles are being carried on rapidly. Changes in engine construction and motor efficiency upgrade studies still continues in our day. For example, Ceramic applications in motors which are parallel to the development of high technology ceramics are rapidly increasing [1]. With the advance in technology, such properties as wear and corrosion resistance are highly demanded in modern industry. Ceramic materials as  $Al_2O_3$ ,  $TiO_2$  and  $ZrO_2$ , have high hardness and strength, chemical stability and acceptable toughness features [2].

For the usage in industry, materials are required to carry some surface properties within their body. Various coating methods are available for this purpose. One is them is the thermal spray technique, a manufacturing technique, used in wide fields for various coating applications [3, 4]. Thermal barrier coatings (TBCs) are widely used to insulate metallic components in gas-turbine engines from high temperatures, which can prolong the lifetime of the component and/or increase the allowable operating temperatures. The two commercial processes used for the deposition of TBCs are air plasma spray (APS) and electron-beam physical-vapor deposition (EB-PVD) [5]. Thermal spray, and particularly atmospheric plasma spray (APS), is one of the most economical and viable processes to obtain coatings at an industrial scale, given its high deposition rates and that there is no need for special atmospheric or chemical chambers. Additional

advantages are the durability and high thickness of the coatings [6]. The low density, high strength, ductility and thermal conductivity of aluminum alloys have provided many applications, particularly in the aerospace and automotive sectors [7].

In this study, the surface of a piston (AlSi12CuNi) belonging to a diesel engine has been coated with  $ZrO_2+MgO$  powder and  $Al_2O_3$  powder mixtures stirred into  $ZrO_2+MgO$  at different rates (25%, 50, 75) using plasma spray technique. SEM, EDS and XRD analysis of samples, hardness and adhesion strength tests and the effect of added  $Al_2O_3$  have been examined after the coating process.

## 2. Materials and method

The chemical composition of piston used as substrate material was given in Table 1, and the data related to coating powders was given in Table 2.  $ZrO_2+MgO$  and  $Al_2O_3$  supplemented coatings have been carried out with the manual use of 3 MB gun in the plasma spray coating units. Plasma spray coating method has been shown schematically in Fig. 1 and plasma spray coating parameters have been given in Table 3. Pictures of the piston before and after the coating are given in Fig. 2. Prior to the coating, the surfaces of the substrate materials to be coated have been subjected to sandblasting in order to increase bond strength of the samples to the surface. Sand blasting process has been carried out by spraying 60 grit  $Al_2O_3$  powder particles to the surface of the substrate material at a  $90^\circ$  angle.

Table 1. The chemical composition of the substrate material to the piston.

Weight (%) Composition					
Al	Si	Ni	Cu	Mg	Fe
Balance	12,6	1,96	0,88	0,60	0,5

Table 2. Particle size of powders used in this study [8].

Plasma spray powders	Sulzer Metco Code	Particle Size ( $\mu\text{m}$ )
ZrO <sub>2</sub> +MgO	210NS	-90 +11
Al <sub>2</sub> O <sub>3</sub>	105NS	-45 +15

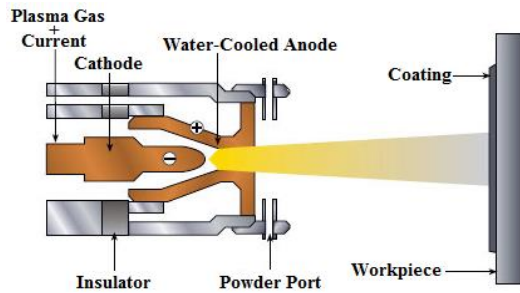


Fig. 1. Schematic cross-section of a typical plasma spray [9].

Table 3. Plasma Spray Coating Parameters.

Parameters	ZrO <sub>2</sub> +MgO/Al <sub>2</sub> O <sub>3</sub>
Plasma Gun	3 MB
Current (A)	500
Voltage (V)	60
Plasma Gas and Flow (l/min)	Ar, 80 H <sub>2</sub> , 15
Spray Distance (mm)	75
Nozzle Diameter (mm)	7,6



Fig. 2. Pistons coated with plasma spray technique.

After the coating process of piston samples, samples prepared at 25.4 mm (1 inch) diameter have been glued to the heads used in tensile testing apparatus using a Scotch-W type thermosetting adhesive made out of resin epoxy and owned by 3M Company for tensile tests. Prepared samples have been dried in the thermo heat furnaces at a temperature of 200 ° C for two hours. By being removed the micro structural sample in cross section perpendicular to the direction of coating, their surfaces have been grinded using 300, 600, 800 and 1200 mesh sanders and then have been polished using diamond paste with broadcloth for micro structural analysis. The microstructures of the specimens were investigated by scanning electron microscopy (SEM), energy dispersive spectroscopy (EDS) and X-ray diffraction (XRD using Cu K $\alpha$  radiation) analysis.

### 3. Results and discussion

SEM images of ZrO<sub>2</sub>+MgO and Al<sub>2</sub>O<sub>3</sub> additional powders coated with plasma spray method are shown in Fig. 3. Layer thicknesses varying between 150 - 300  $\mu\text{m}$  have been obtained in plasma spray coatings applied on piston (AlSi12CuNi) surface. Porosity has been found in all of the coatings carried out with different powders. Porosity is a traditional structure of plasma spray coatings [3, 10, 11]. The lowest amount of the porosity, as seen in microstructure pictures, has been identified in samples coated with ZrO<sub>2</sub>+MgO+%50Al<sub>2</sub>O<sub>3</sub>. When coating layers and substrate material interfaces have been analyzed, no gaps, cracks and oxidation has been found. The absence of gaps, cracks and oxidation has a positive impact on the adhesion strength.

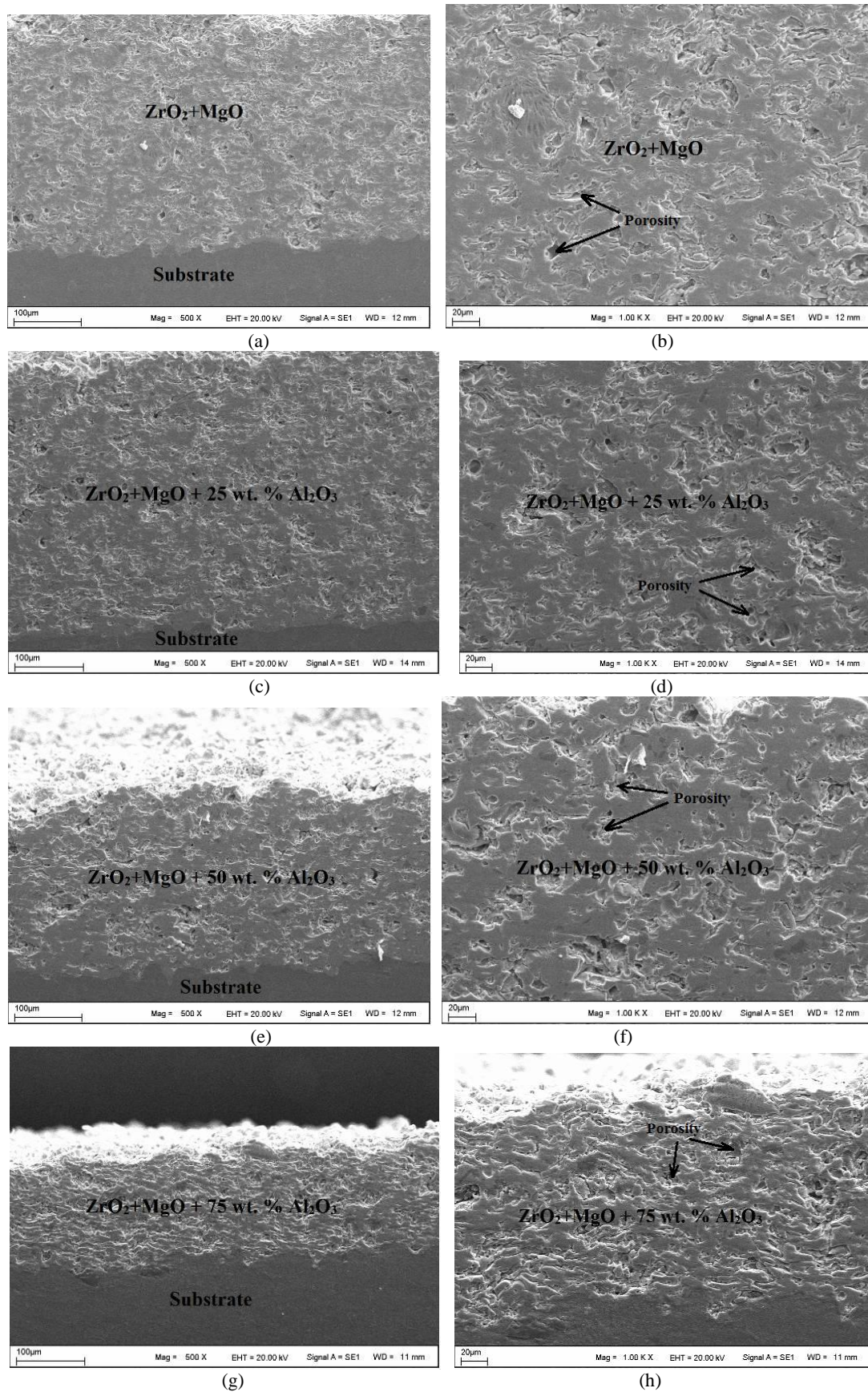
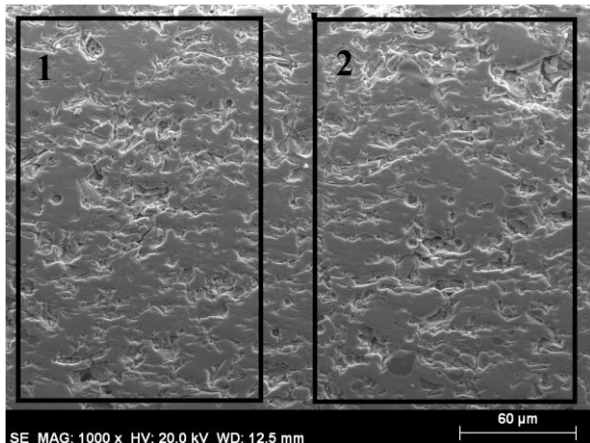
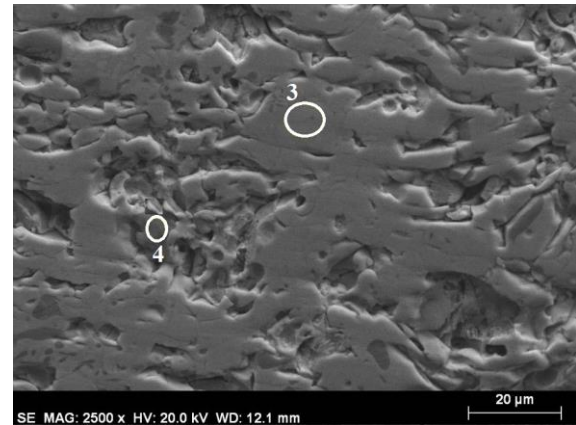


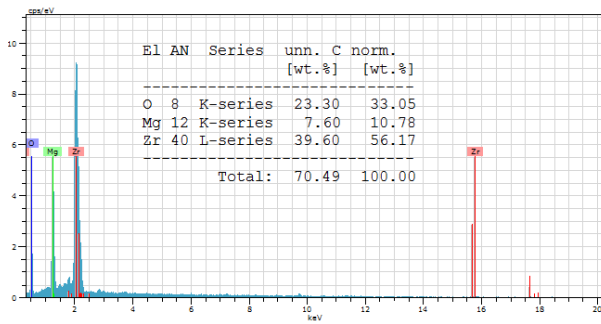
Fig. 3. SEM Microstructure of  $ZrO_2+MgO/Al_2O_3$  coatings, a,b)  $ZrO_2+MgO$  coated, c,d) 25 wt. %  $Al_2O_3$  added, e,f) 50 wt. %  $Al_2O_3$  added g,h) 75 wt. %  $Al_2O_3$  added.



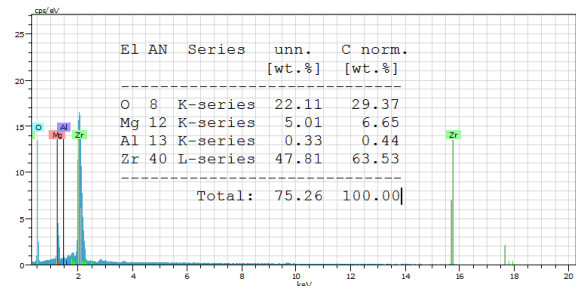
(a)



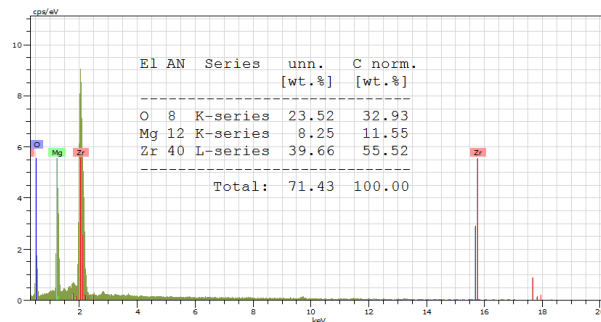
(a)



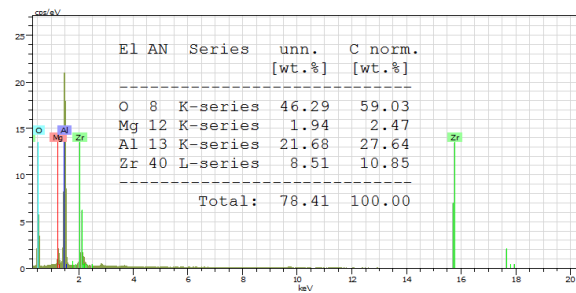
(b)



(b)



(c)



(c)

Fig. 4. SEM photo and EDS analyses of specimen coated with  $ZrO_2+MgO$  powder.

EDS analysis and SEM microstructure pictures taken from coating layer coated with  $ZrO_2+MgO$  powder are shown in Fig. 4. Percent (wt. %) values of Zr, Mg and O elements are seen in EDS analysis results. In EDS analysis (Fig. 4-b) taken from the zone number 1 and sample's coating layer coated with  $ZrO_2+MgO$  powder highly 56.17wt.%Zr, 10.78wt.%Mg, 33.05wt.%O elements and in the EDS analysis taken from the zone number 2 (Fig. 4-c) 55.52wt.% Zr, 11.55wt.%Mg, 32.93wt.%O elements have been determined. These values show that coating layer is made of zirconium oxide and magnesium oxide compounds. XRD analysis result of a sample given in Fig. 6 verifies these compounds.

Fig. 5. SEM photo and EDS analyses of specimen coated with  $ZrO_2+MgO+50\text{ wt. \% }Al_2O_3$  powder.

EDS analysis and SEM microstructure pictures taken from coating layer of a piston coated with  $ZrO_2+MgO+50\text{ wt. \% }Al_2O_3$  powder are shown in Fig. 4-1. Percent (%) values of Zr, Mg and O elements are observed in EDS analysis results. In EDS analysis (Fig. 5-b) taken from the zone number one and sample's coating layer coated with  $ZrO_2+MgO+50\text{ wt. \% }Al_2O_3$  powder highly 63.53wt.%Zr, 29.37wt.%Mg, 0.33wt.%Al and 29.37wt.%O elements have been determined. When these values are analyzed it has been seen that zone number 3 has more zirconium oxide and magnesium oxide compounds. In EDS analysis (Fig. 5-c) taken from the zone number 4 highly 10.85wt.%Zr, 0.33wt.%Al, 11.55wt.%Mg, 32.93wt.%O elements have been determined. These values show that coating layer consists of zirconium oxide and magnesium oxide and aluminum oxide. XRD analysis result of a sample given in Fig. 6 verifies these compounds.

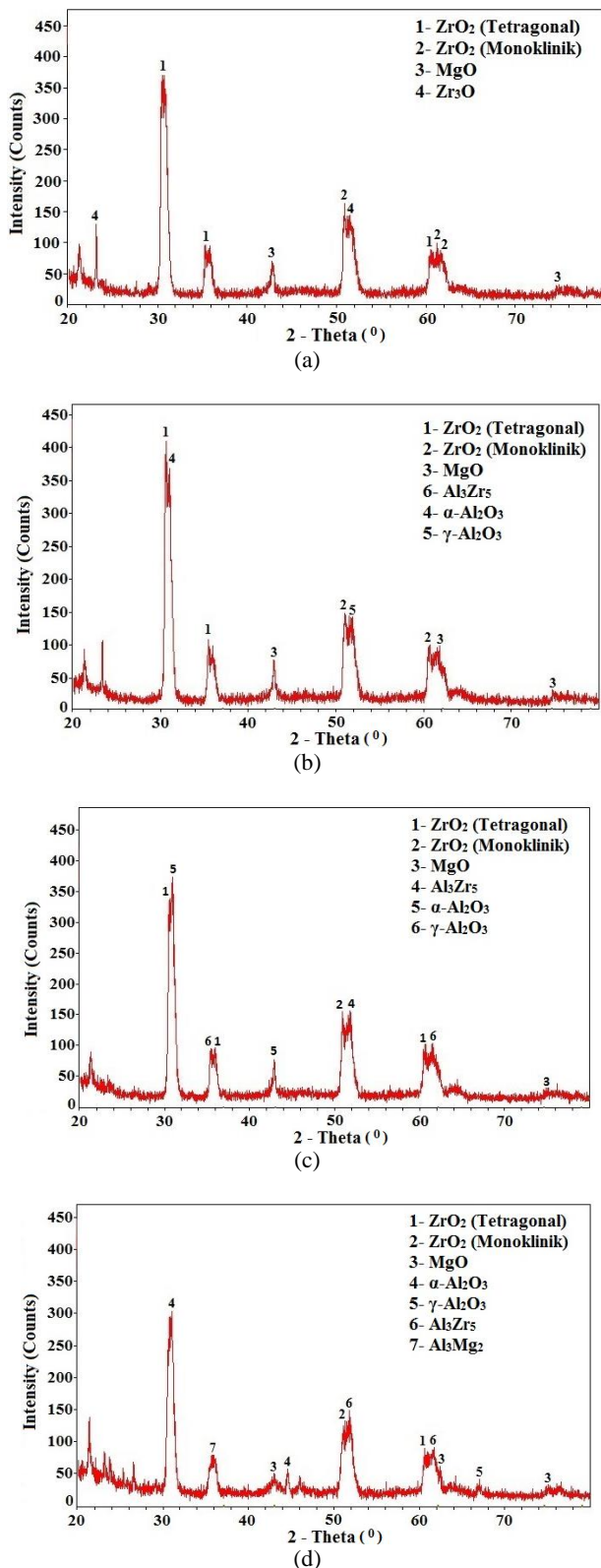


Fig. 6. XRD patterns of ZrO<sub>2</sub>+MgO / Al<sub>2</sub>O<sub>3</sub> coated specimens, a) ZrO<sub>2</sub>+MgO b) 25 wt. % Al<sub>2</sub>O<sub>3</sub> added, c) 50 wt. % Al<sub>2</sub>O<sub>3</sub> added, d) 75 wt. % Al<sub>2</sub>O<sub>3</sub> added.

XRD analysis taken from the coating layers of the samples coated with Al<sub>2</sub>O<sub>3</sub> addition and ZrO<sub>2</sub>+MgO are shown in Fig. 6. In ZrO<sub>2</sub>+MgO and Al<sub>2</sub>O<sub>3</sub> additional

coatings ZrO<sub>2</sub> (Tetragonal), ZrO<sub>2</sub> (Monoklinik), MgO, Al<sub>3</sub>Zr<sub>5</sub>, Al<sub>3</sub>Mg<sub>2</sub>, α-Al<sub>2</sub>O<sub>3</sub> and γ-Al<sub>2</sub>O<sub>3</sub> compounds have been identified. Zirconia (ZrO<sub>2</sub>) is monoclinic (m-ZrO<sub>2</sub>) below 1170 °C, tetragonal (t-ZrO<sub>2</sub>) up to 2370 °C, and then cubic (c-ZrO<sub>2</sub>) at high temperature up to the melting point (2680 °C) [12, 13].

Phase Al<sub>3</sub>Zr<sub>5</sub>, as can be inferred from binary phase diagram Al-Zr [14], is a high-temperature phase. It may form Al<sub>3</sub>Zr<sub>5</sub> and different inter metallic phases depending on the solidifying temperature at the binary phase diagram [15, 16]. As can be inferred from Al-Mg binary phase diagram, Al<sub>3</sub>Mg<sub>2</sub> intermetallic compound comprises when temperature is above 450 °C [17].

The reason of α-Al<sub>2</sub>O<sub>3</sub> and γ-Al<sub>2</sub>O<sub>3</sub> depends on the conditions of plasma spray coatings and heat conditions during the cooling process. When Al<sub>2</sub>O<sub>3</sub> calcined at high temperatures, it transforms into a hexagonal crystal structure with an α form. The other crystal structure of Al<sub>2</sub>O<sub>3</sub> is an orthorhombic system shown as γ - Al<sub>2</sub>O<sub>3</sub>. γ - Al<sub>2</sub>O<sub>3</sub> also transforms into α - Al<sub>2</sub>O<sub>3</sub> structure at a temperature 927 °C [18, 19].

#### 4. Microhardness and bonding strength

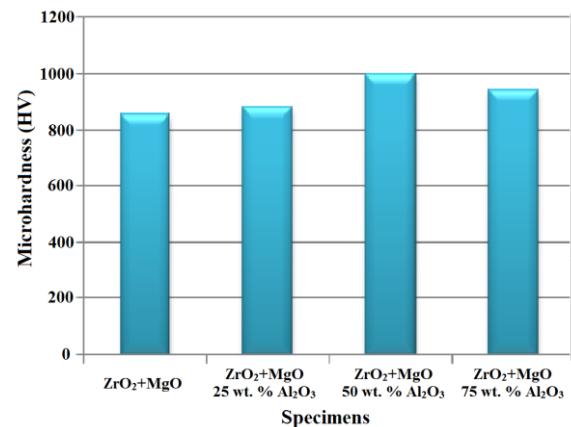


Fig. 7. Microhardness of plasma spray coatings.

Microhardness results of the coatings made ZrO<sub>2</sub>+MgO and Al<sub>2</sub>O<sub>3</sub> additional powders are shown in Fig. 7. In the sample coated with ZrO<sub>2</sub> + MgO, changing between 750 HV and 780 HV, in the sample coated with ZrO<sub>2</sub> + MgO + 25 wt. % Al<sub>2</sub>O<sub>3</sub> between 770 HV and 800 HV, in the sample coated with ZrO<sub>2</sub> + MgO + 50 wt. % Al<sub>2</sub>O<sub>3</sub> between 950 HV and 1000 HV and in the sample coated with ZrO<sub>2</sub> + MgO + 75 wt. % Al<sub>2</sub>O<sub>3</sub> between 850 HV and 950 HV microhardness values have been measured. With the increase of added Al<sub>2</sub>O<sub>3</sub> rate to the coatings, an increase in the microhardness value has been determined. But, despite the highest Al<sub>2</sub>O<sub>3</sub> rate in the sample coated with ZrO<sub>2</sub> + MgO + 75 wt. % Al<sub>2</sub>O<sub>3</sub>, microhardness in the sample coated with %50 Al<sub>2</sub>O<sub>3</sub> addition is higher due to the low porosity rate of the sample coated with 50 wt. % Al<sub>2</sub>O<sub>3</sub> [1, 2, 3]. The highest hardness value has been measured as 996 HV in the sample coated with ZrO<sub>2</sub> + MgO + 50 wt. % Al<sub>2</sub>O<sub>3</sub>.

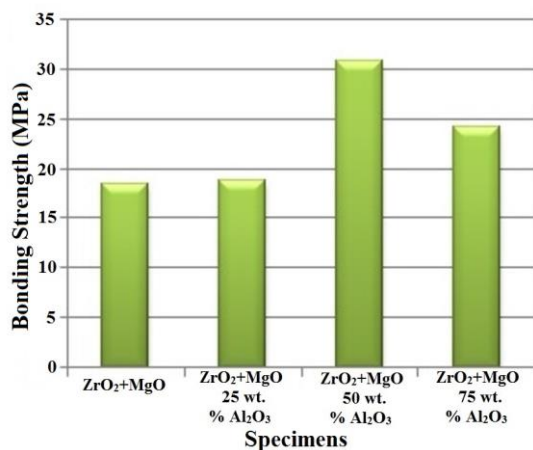


Fig. 8. Bonding strength of plasma spray coatings.

Graph showing the post tensile test adhesion strength that belongs to coated samples with ZrO<sub>2</sub> + MgO and Al<sub>2</sub>O<sub>3</sub> additional powder are shown in Fig. 8. When graphic is analyzed, the adhesion strength is seen to increase with Al<sub>2</sub>O<sub>3</sub> addition. The high adhesion strength has been obtained with a 30.83 MPa rate in the coatings made with ZrO<sub>2</sub> + MgO + 50wt. % Al<sub>2</sub>O<sub>3</sub> powder. Compared to the sample coated with adding 75wt. % Al<sub>2</sub>O<sub>3</sub>, the increase of adhesion strength of the sample coated with adding 50% Al<sub>2</sub>O<sub>3</sub> is due to the low porosity in the coatings prepared adding 50wt. % [18].

## 5. Conclusions

In this study, the surface of a piston (AlSi12CuNi) belonging to a diesel engine has been coated with ZrO<sub>2</sub>+MgO powder and Al<sub>2</sub>O<sub>3</sub> additional powder mixtures stirred into ZrO<sub>2</sub>+MgO at different rates (wt. % 25, 50, 75) by using plasma spray technique. The following results have been obtained after the surface roughness and adhesion strength tests, EDS and XRD analysis, SEM microstructure analysis of the coated layers.

- 1- A porous structure has been attained from all of the coatings. Al<sub>2</sub>O<sub>3</sub>, ZrO<sub>2</sub> and MgO zones have been identified though EDS analysis within the coating layer. No gap, cracks and oxidation have been identified between the coating layer and the substrate material.
- 2- ZrO<sub>2</sub> (Tetragonal), ZrO<sub>2</sub> (Monoclinic), MgO, Al<sub>3</sub>Zr<sub>5</sub>,  $\alpha$ -Al<sub>2</sub>O<sub>3</sub> and  $\gamma$ -Al<sub>2</sub>O<sub>3</sub> compounds have been identified in ZrO<sub>2</sub>+MgO and Al<sub>2</sub>O<sub>3</sub> additional coatings.
- 3- In micro hardness analysis, an increase in the microhardness has been identified in the coatings prepared adding Al<sub>2</sub>O<sub>3</sub>. The highest microhardness value, 996 HV, has been identified in the sample coated adding 50wt.% Al<sub>2</sub>O<sub>3</sub>
- 4- The highest adhesion strength, 30.83 MPa, has been identified in the sample coated with ZrO<sub>2</sub> + MgO + 50wt.% Al<sub>2</sub>O<sub>3</sub> where porosity level is the lowest.

As a result of the this analysis, among the ZrO<sub>2</sub>+MgO/Al<sub>2</sub>O<sub>3</sub> coatings applied on the motor piston,

the best results are achieved in ZrO<sub>2</sub>+MgO+50wt.% Al<sub>2</sub>O<sub>3</sub> coated samples.

## Acknowledgements

This work was supported by Scientific Research Project Unit of Karabuk University under project-No: KBU-BAP-13/2-DR-004. The authors would like to thanks the Bitlis Eren University Science and Technology Research and Application Center for tests of specimens and Turkish Airlines Technic Inc. for the coatings with bonding strength tests.

## References

- [1] J. A. Gataowski, Society of Automotive Engineers, USA (1990).
- [2] Y. Yang, D. Yana, Y. Donga, X. Chena, L. Wang, Z. Chua, J. Zhanga, J. He, *Vacuum*, **96**, 39 (2013).
- [3] S. Özel, H. Turhan, F. Sarsilmaz, *Firat University, Journal of Science and Engineering*, **3**, 503 (2008).
- [4] R. C. Tucker, *Thermal Spray Coatings*, **5**: Surface Engineering, ASM Handbook, Ohio (1994).
- [5] M. Gell, L. Xie, E. H. Jordan, N. P. Padture, *Surface and Coatings Technology*, **188–189**, 101 (2004).
- [6] M. Vicent, E. Banniera, R. Morenob, M. D. Salvadorc, E. Sáncheza, *Journal of the European Ceramic Society*, **33**(15–16), 3313 (2013).
- [7] Y. Baoa, D. T. Gawne, J. Gaoa, T. Zhang, B. D. Cuenca, A. Alberdi, *Surface and Coatings Technology* **232**, 150 (2013).
- [8] [www.sulzer.com/ThermalSprayMaterialsGuide\(13.03.2014\)](http://www.sulzer.com/ThermalSprayMaterialsGuide(13.03.2014)).
- [9] S. Özel, H. Turhan, *Materials Testing*, **52**, 4 (2010).
- [10] A. Portinha, V. Teixeira, J. Carneiro, J. Martins, M. F. Costa, R. Vassen, D. Stoeber, *Surface & Coatings Technology*, **195**, 245 (2005).
- [11] A. Kucuk, C.C. Berndt, U. Senturk, R. S. Lima, *Materials Science and Engineering, A*, **284**, 41(2000).
- [12] S. Özel, PhD Thesis, *Firat University*, 1-149 (2009).
- [13] C. Salle, P. Grosseau, G. Bernard, P. Iacconi, M. Benabdesselam, G. Fantozzi, *Journal of the European Ceramic Society*, **23**, 5, 667-73 (2003).
- [14] C. Li, J. She, M. Pang, W. Yang, Y. Zhan, *Journal of Phase Equilibria and Diffusion*, **32**, 1 (2011).
- [15] J. Shea, Y. Zhan, C. Lia, Y. Du, H. Xu, Y. He, *Journal of Alloys and Compounds*, **503**(1), 57 (2010).
- [16] H. Okamoto, *Journal of Phase Equilibria*, 455–456 (2002).
- [17] D. H. Choia, B. W. Ahna, D. J. Quesnelb, S. B. Jung, *Intermetallics*, **35**, 120 (2013).
- [18] A. F. Taggart, *Handbook of Mineral Dressing-Taggart, Ores and Industrial Minerals*, Wiley Handbook Series, John Wiley-Sons Inc., New York (1945).
- [19] G. Gulfen, *The solubility of Milas Bauxite Ore in Hydrochloric Acid Solution*, M. Sc. Thesis, Sakarya University, (1998).

\*Corresponding author: sozel@beu.edu.tr